CHAPTER VII

DISCUSSION

In an attempt to understand neotectonism in this study area all of information in past sections are integrated in order to discuss in this chapter. Discussing issues in this study consist of neotectonic feature, tectonic stress field, earthquake recognition, classification of active fault, and seismic hazard assessment. The results of discussion are cited below.

7.1 Neotectonic Features

Based on Landsat TM and JERS imagery data, the Phrae fault system can be divided into four segments, the southwestern, the western, the southeastern and the northeastern segments. However, according to previous studies, there was no proposed any detailed study on fault segmentation before.

Neotectonics features of the southeastern segment have been clarified. The southeastern segment of the Phrae fault system is delineated in NNE-trending with approximately 20 km long. This segment characterizes as basin-bounded fault since the fault trace is located closed to the southeastern margin of the Phrae basin and situated between mountain range front and the basin area.

Depending on aerial photograph interpretation, the southeastern segment can be further subdivided into three subsegments, ranging from the south to the north; which are Ban Thung Charoen, Ban Kwang, and Ban Pa Daeng subsegments. According to morphotectonic interpretation using aerial photograph, there are several fault branches observed containing in the principal displacement zone of the segment. Major trend of the fault branches lies in NNE and the minor in ENE.

The southeastern segment tracing from seismic profiles interpreted by Srisuwan et al (2000) and Khrauthao (2001), which is so-called eastern border fault, revealed some controversy. There are three lines of seismic profiles which run across the present thesis area. Line nos. P94-220, P94-240, and P94-260, run through the northern, the central, and the southern part of the thesis area, respectively. In line no. P94-220, Srisuwan et al. (2000) reported the existence of eastern border fault whereas Khrauthao (2001) did not report as such. Unfortunately, Srisuwan et al. (2000) did not report the result of line no. P94-240. However, the

eastern border fault delineation in seismic line no. P94-260 is quite the same. Besides, depending on seismic interpretation resulting from this present study, the interpreted fault resembles that of Srisuwan et al. (2000) since both results yield eastern border fault in line nos. P94-220 and P94-260. Subsequently, it can be cited herein that based on seismic profiles, remote-sensing, and aerial photographic interpretations, the southeastern segment or the eastern border fault is definitely located on the southeastern portion of the Phrae basin, dip-to-the west with 45 degrees.

Three evidences of tectonic geomorphology were found along the southeastern segment trace. Two of these evidences are a shutter ridge and triangular facets found along the trace of Ban Kwang subsegment. These evidences are clearly defined on both aerial photograph and field investigation. The evidences indicate that Ban Kwang subsegment was once displaced with left-lateral and normal movements. The movements may have taken place in the same event or vice versa. The other evidence of fault movement is two offset stream channels as defined by using aerial photograph method. This method is advantage to delineate offset stream channel rather than ground-truth survey. These tectonic evidences are located to be closed to the southeastern end of basin margin. The stream channels had been found offset by the fault trace of Ban Thung Charoen subsegment with left-lateral displacement. In addition, six outcrops on high terrace, which lie along and close to the eastern mountain range front, had been explored to be deformed by small normal faulting. Almost all faults are east-dipping cut across west-dipping tilt layers. Depending on seismic profile line no. P94-240, the small fault shows antithetic and conjugate characteristics to the eastern border fault. If the eastern border fault is the major fault, the small normal faults are inferred to be the minor antithetic faults. Due to its distance is too closed, the major and minor antithetic faults are believed to have a closed genetic relationship to each other in term of movement characteristics. However, the minor fault trace is not found continued as a single trace but characterized as small fault branches. There is no evidence of antithetic minor fault in seismic profile line nos. P94-220 and P94-260 since these lines were not run across fault branches.

In contrast, Fenton et al.(1997) and GMT (1995a) cited that there was no evidence of eastern border fault found on both seismic profile and tectonic geomorphology. These authers had found only one outcrop of normal fault cut across high terrace in landfill nearby Ban Pa Daeng2

outcrop. Therefore, they had interpreted that this fault is synthetic fault of the western border fault.

Based on the results of the field study, Ban Thung charoen and Ban Kwang subsegments have characterized as normal-sinistral motion. In Ban Pa Daeng subsegment, unfortunately, only the evidence of normal motion from high terrace outcrop had been found. However, these subsegments are located to be closed to each other, and all of these have short fault lengths. Therefore, its displacement should be in analogous sense. Nevertheless, the results from earthquake fault plane solutions in northern Thailand especially near Rong Kwang event in December 9, 1997 revealed that contemporary movement of the NE-trending fault in this province is in left-lateral with small component of normal movements. Therefor, if the southeastern segment still active, all subsegments should be undergoing with the same normal-sinistral movement. This study is found consistent to Srisuwan et al (2000) in term of location and sense of movement of the southeastern segment. However, Charoenprawat et al. (1995) stated that eastern border fault of the Phrae basin was determined as right-lateral fault based on the offset of Triassic rocks (TR7 unit). Chauviroj (1995) also noted that the Phrae fault zone characterized as a dextral displacement fault.

Based on tectonic stress field study, which had discussed in section 7.2, there are at least two episodes of tectonic stress orientations are recognized. The first episode indicated by approximately N-S trending of T-axis. The second or contemporary episode has revealed about E-W trending of T-axis. This study in conjunction with Charoenprawat et al.(1995) and Chauviroj (1995) results, it can be interpreted that TR7 unit which was offset by right-lateral movement of the NE to NNE fault, was taken place during the first episode, for the sense of fault movement corresponds to T-axis. However, left-lateral and normal movements that observed along the southeastern segment are believed to be the results of the second episode or the contemporary stresses.

Based on remote-sensing study, aerial photographic interpretation, seismic reflection profiles, and field observation, conceptual block diagram of the southeastern segment of the Phrae fault system can be constructed as shown in Figure 7.1.

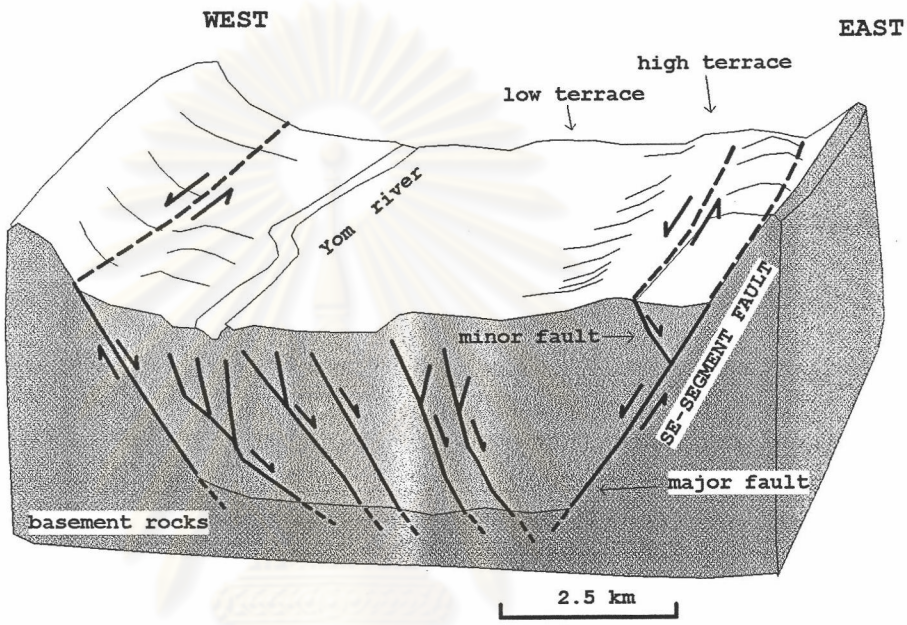

Figure 7.1 Schematic block diagram of southern portion of the Phrae basin. The southeastern segment is located at the eastern border of the basin.

7.2 Tectonic Stress Field

In this section, tectonic stress axis orientation has been discussed, particularly contemporary stresses. Focal mechanism study and stress axis reconstruction using field evidences including fault and joint data are of an attempt in this current study. In addition, previous study on the context related to this issue is also integrated to discuss in this section.

According to focal mechanism solution of near Rong Kwang earthquake event (M_W 5.1), which was taken place in December 9, 1995. For the recent study, the result shows that contemporary maximum principal stress or compressional stress axis (P-axis) is found in NNE-SSW whilst minimum principal stress or tensional axis (T-axis) is in ESE-WNW direction. Both axes are found acting in sub-horizontal plane with 15 and 14 degree of plunge. This earthquake event was contributed by strike-slip movement with small normal component.

This study result is similar to focal mechanism solution of the same event constructed by Bott et al. (1997) in term of stress axis orientation. Moreover, the previous study on contemporary stress axis orientation in northern Thailand by Bott et al. (1997) had suggested that northern Thailand is undergoing approximately east-west orientation of tensional stress axis in active normal and oblique-slip movements. Three focal mechanisms of past moderate earthquakes in northern Thailand are consistent with geological data, which contribute comprehensive knowledge that this region is undergoing east-west to northwest-southeast extension on north- to northeast-striking normal or normal-oblique faults (Fenton et al, 1997). In the report of dextral transtensional shear model by Polachan & Sattayarak (1989), two principal stress elements are composed of north-south compression and east- west extension of present-day tectonic stress axis orientation in Thailand. They also stated that the NW-SE trending such as the Red River, the Mae Ping, The Three Pagodas, and the Sumatra faults are the principal dextral faults, whereas the NNE-SSW trending included the Northern Thailand, the Uttaradit, the Ranong, and the Klong Marui faults are the conjugate sinistral faults, which are found terminated to the dextral faults. These previous works are consistent to this thesis result on the focal mechanism solution. Consequently, based on all results stated above the southeastern segment of the Phrae fault system, which is delineated in NNE-SSW trending, should be undergoing normal-sinistral movement.

Additionally, as the results of fault and joint analyses using field data constructed on stereogram, these sets of data yield three sets of results. They included fault analysis using fault data from high terrace outcrop, joint analysis using joint data observed at Ban Pa Daeng high terrace outcrop, and joint analysis using joint data from hard rock outcrop in mountainous area nearby Mae Man reservoir. Fault analysis reveals extension axis in the ESE-WNW trend. Ban Pa Daeng joint analysis suggests that tensional axis lies in approximately E-W trending whilst compressional axis is in about N-S trending. Rock-preserved joint analysis shows that compressional and extensional axes are determined in about E-W and N-S trending, respectively. Based on these analyses, it can be proposed that stress axis orientation in this area has been changed at least in two episodes. The first episode is determined by roughly N-S orientation of extensional axis due to rock joint data analysis. This result is consistent with past right-lateral offset of Triassic rock of Ban Kwang subsegment, which is inferred to be the resultant of N-S extension. The second episode is change from the first to about E-W orientation of extensional axis referred from fault and joint data of high terrace outcrops. However, there is no joint orientation as preserved in Ban Pa Daeng1 outcrop had found in that hard rock outcrop. This question may be explained that after the second episode and the stress axis orientation has changed, faulting events have generated only small to moderate magnitudes of earthquakes. These earthquakes could not created new set of joint in hard rock, which is located up to the ground surface as deduced by the decrease of stress from hypocenter. However, on the high terrace outcrops, which are composed of semi-consolidated to consolidated sediments. Their strength is much lower than Triassic rock, therefore earthquakes could create joint sets easier than in the hard rocks.

Folding which found closed to the right side of Ban Pa Deang1(PDR)outcrop is believed to be occurred by $\sigma 2$ moderate compressional force of PDR outcrop (see Figure 5.9). On the other hand, $\sigma 2$ that created faulting in PDR outcrop is also the maximum force ($\sigma 1$) that created folding.

Based on this result, two episodes of stress axis orientation can be summarized as simplified strain ellipsoid illustrated in Figure 7.2.

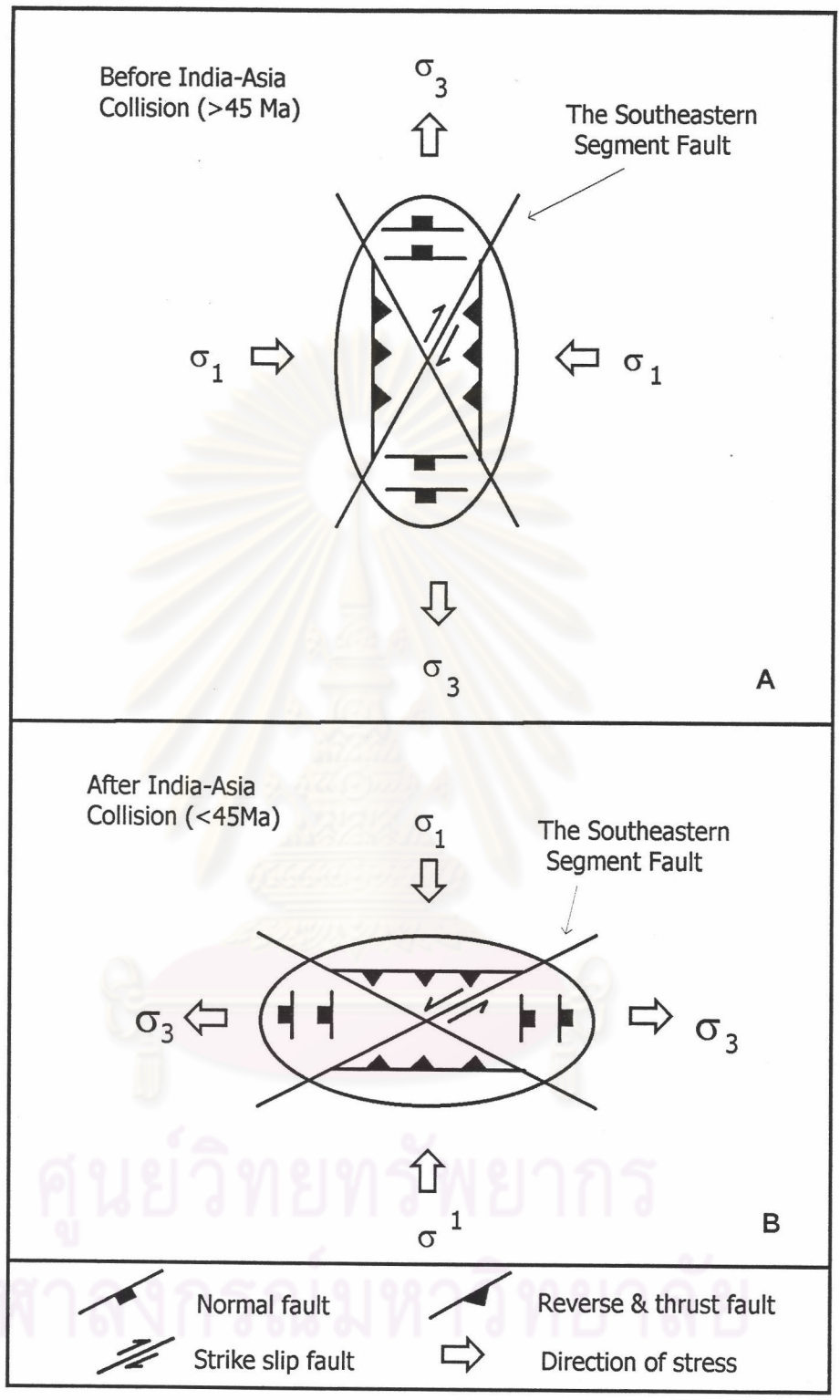

Figure 7.2 Simplified strain ellipsoids of two episodes; before India-Asia collision (A) and after India-Asia collision (B). Open arrow with σ1 indicates compression direction, and open arrow with σ3 indicates extension direction of tectonic forces. The southeastern segment of the Phrae fault system had a dextral movement before India-Asia collision and has a sinistral movement since India-Asia collision.

7.3 Earthquake Event Recognition

No exposures of neotectonic evidence of stratigraphic deformation such as faulting, jointing and folding had been observed along the major fault trace of the southeastern segment. Nevertheless, these evidences were investigated in six outcrops of high terraces. The terraces are overlying along eastern margin of the Phrae basin, with about 1 km between the terraces and eastern mountain front. These normal faults are inferred to be the minor faults, antithetic to the major southeastern segment fault (see Figure 7.1). Displacement found on the minor faults is believed to be mainly created by the major fault. Therefore, earthquake event evaluation from the minor faults might be represent the major fault.

As a result, two events of moderate to large earthquakes interpreted from normal fault and fracture evidences from high terraces (Figure 7.3). Based on these evidences and TL-dating results, earthquake events are

event1, between 0.890 Ma and 1.10 Ma, and

event2, between 0.050 Ma and 0.170 Ma.

For event1, in Ban Pa Daeng1 outcrop, age of earthquake event is inferred between unfaulting and faulting layers. This evidence is characterized on two sides of the outcrop. The left side one yields their age interval between 0.480 and 1.200 Ma. The right side reveals age interval between 0.890 Ma and 1.100 Ma (see Figure 7.3C).

According to these evidences, the similar characteristic was found located in the same outcrop, thus it should be produced by the same event. On account of the age interval derived from the right side outcrop is in between age interval derived from the left side outcrop, therefore, this event should have occurred between 0.890 Ma and 1.100 Ma as inferred from the right side.

Regarding to the TL-dating result from Chom Chaeng1 outcrop in this recent study, a sedimentary sample collected from faulting layer yields its TL-age 0.170 Ma. This result is consistent with TL-dating result carried out by Won-in (2002). Won-in (2002) revealed three dating results of sediments from the same outcrop. The first result is 0.060 Ma, which is the age of the upper layer compared to this recent study. However, this layer had no evidence of offset by fault. The second sample collected

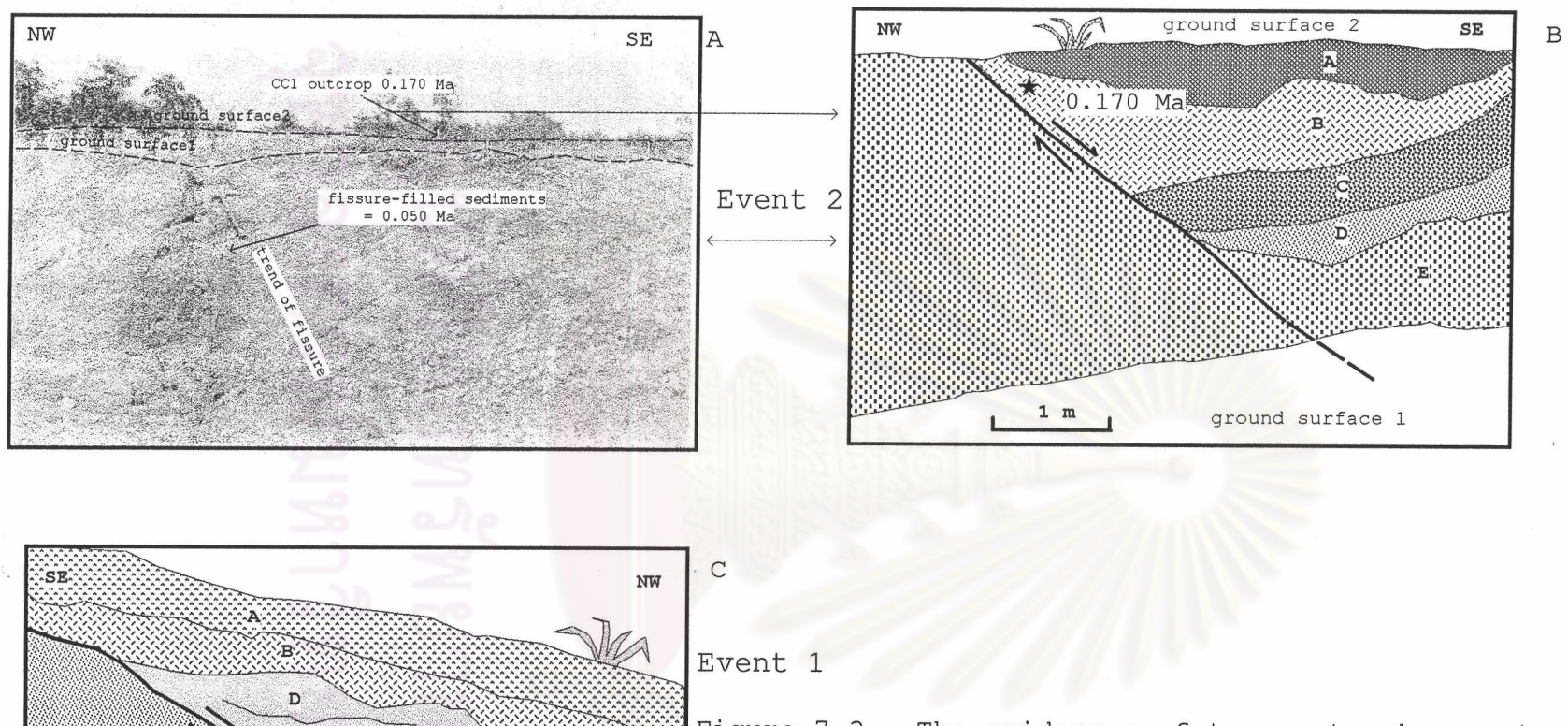

Figure 7.3 . The evidences of two eartquake events in the study area. The first event took place during 0.890 Ma and 1.100 Ma, as evidenced at the right side of the Pa Daeng1 outcrop (C). The second event occured during 0.050 Ma, and 0.170 Ma, as evidenced at the Chom Chaeng1 outcrop (A and B).

from the lower layer of this study, found the age of 0.280 Ma. Finally, the last sample is fracture-filled sediments yields the TL-age of 0.050 Ma. Additionally, fracture orientation lies in the same trend of the fault, then these fractures are inferred to be created by the same event. Subsequently, fracture-filled sediments is referred to be deposited after faulting. Therefore, this faulting or earthquake event must be occurred between ages of faulting layer and fracture-filled sediments, which is between 0.050 Ma and 0.170 Ma (see Figure 7.3 A&B).

In Ban Thung Charoen outcrop, the dating revealed by this thesis has provided its age of faulting event in this outcrop to occur before 1.300 Ma, as determined from age of undeformed sedimentary layer that overlain faulting layers. However, depending on TL-dating results of sediments in the faulting layer by Won-in (2003), ranging from upper, middle, and lower layers, they are 0.600 Ma, 0.660 Ma and 0.990 Ma, respectively. Regarding to Won-in (2003), the dating results are consistent to one another. Unfortunately, these results are non-consistent to the result of this thesis study. Since dating results of Won-in (2003) are more orderly conformable than that of this thesis study, so based on his results, this earthquake event should have occurred after 0.600 Ma.

7.4 Classification of Active Faults

According to the existence of two components of conjugate fault of the southeastern segment of the Phrae fault system, the major fault and minor fault are obvious (see Figure 7.2). The raw data for active fault classification were collected from both faults. As a result, there was no evidence and report on historical surface offset of tectonic fault. However, one moderate to large earthquake had occured within 100,000 yrs, according to paleoseismological study. Moreover, subdued, eroded and discontinuous tectonic geomorphology of triangular facets, a shutter ridge, and offset stream channels were observed along the major fault trace. In addition, faults offset Pleistocene high terraces were also found along the minor fault trace. Subsequently, based on classification of active fault by Charusiri et al.(2001), the southeastern segment of the Phrae fault system is classified as a potentially active fault.

In the report of Nutalaya (1986), it suggested that the Phrae fault zone is probably active but more evidences on both seismicity and geology is required

before definite conclusion. The Phrae fault zone in this report is referred to the major fault of the present study. The recent study has collected both seismic and geological data, as Nutalaya (1986) recommended, for active fault classification, and finally concluded that it is the potentially active fault.

GMT (1995b) mentioned that east-dipping normal faults, which cut across young basin-fill sediments, are active. These faults are referred to the minor fault of this thesis study. Fenton et al. (1997) revealed that the Phrae basin fault is active fault. This fault is also referred to the minor fault of this thesis study. Note that both GMT (1995b) and Fenton et al. (1997) had not reported on criteria used for active fault classification. However, this thesis study has more details on both raw data and criteria for classification.

Charurisi et al. (2001) announced that the Phrae fault is rank as active fault which referred to the whole Phrae fault system. However, this thesis study has classified only the southeastern segment which is not represent the whole Phrae fault system. Therefore, the result of this study is not required to similar to the study of charusiri et al. (2001).

7.5 Seismic Hazard Assessments

Since 1960s, government regulations in several industrialized countries have used seismic hazard assessments for construction of new critical structures (e.g., nuclear power plants, dams, hospitals, and schools). Seismic source characterization, which comprises of paleoearthquake magnitude assignment and recurrence of large, potentially damaging earthquake of active fault nearby the site, is a key element for seismic hazard assessments (McCalpin, 1996).

For faults with abundant historical seismicity, large historic surface rupture and monitored strain rates (e.g., the San Andreas fault zone, California, see Schwartz & Coppersmith,1984), paleoseismic data provided additional information of large earthquakes. In contrast, for historical quiescent faults (e.g., the Wassatch fault zone, Utah, see Schwartz & Coppersmith,1984) paleoseismic data provide fruitful information of location, size, and recurrence of large earthquakes which are useful for seismic source characterization.

In this section, three topics related to seismic hazard assessments have been discussed. The first topic

cited on estimation of paleoearthquake magnitude, which took place by the faults in the study area. The second topic mentioned about slip rate of the faults. Finally, earthquake recurrence has been discussed in the last topic.

As previously mentioned with using both satellite imageries and seismic profiles, distance between the minor fault and the major fault (the southeastern segment) is shortest, as about 0.5-1.0 km, as compared to other faults in the Phrea basin. Additionally, seismic line no. P94-240 (see section 3.2) shows the bottom end of the minor fault terminated at the major. This suggests that the major fault movement is believed to be subjected to the displacement on the minor.

Consequently, paleoearthquake magnitude, slip rate, and earthquake recurrence estimations in the following section of the minor faults, in turn, are also referred to the major fault.

7.5.1 Paleoearthquake Magnitude Estimation

Regarding to paleoearthquake magnitude estimation, in this study, maximum displacement method has been applied to find out the magnitudes. Maximum displacement method involves determining the maximum displacement (MD) related to paleoeartquake, and comparing that value to the maximum displacement measured in historic earthquakes (Bonilla et al., 1984; Wells & Coppersmith, 1994)

Wells & Coppersmith (1994) revealed equation for paleoearthquake magnitude estimation, which can be used for all types of faults as below;

$$M = 6.69+0.74x\log (MD)$$

where

M = moment magnitude

MD = maximum displacement.

Three normal faults from three outcrops were selected for evaluating paleoeartquake magnitudes in this area. These three faults have high slip length which are at least 3.0 m, corresponding to the equation used that need maximum displacement parameter.

The result which is based on maximum displacement method shows magnitude between M_w 6.8 and 6.9 (Table 7.1). However, Fenton et al. (1997) estimated paleoearthquake

magnitude using the surface rupture length for the Phrae basin fault, from the minor fault of this study, with an almost similar result of M_w 7.0. Fenton et al. (1997) applied surface rupture length method for this task while this recent study applied maximum displacement method. On account of no faulting surface rupture evident in the study area, therefore, Fenton et al. (1997) assumed its rupture length from the mapped fault trace which may cause over estimation. Nevertheless, both this study results and Fenton et al. (1997)'s result are similar since the results revealed large paleoearthquake magnitudes within the Phrae basin.

7.5.2 Slip Rates

Slip rates are calculated from the cumulative offset of dated deposits or landforms (McCalpin, 1996).

In this study, three faults from three outcrops which have high slip lengths were used to calculate their slip rate as shown in Table 7.1, the result reveals 0.06 mm/yr of slip rate for the antithetic minor fault.

Up to present, only the works of Fenton et al.(1997) had provided slip rate result of the faults in this area.

Fenton et al. (1997) stated that the Phrae basin fault (the minor fault in this study) has 0.1 mm/yr of slip rate determined from paleoseismic trench excavations.

Differentiation between this study and Fenton et al. (1997)'s results should be arisen from age of movement. Since Fenton et al. (1997) used the age Late Pleistocene (0.01 Ma) but this study applies 0.054 Ma for slip calculation.

7.5.3 Recurrence Estimation

There were two moderate to large earthquake events took place in the study area. Fault in Ban Pa Deang1 outcrop (PDR) is inferred to be displaced in the first event. Age interval of this event is 0.890 to 1.100 Ma, with the mean earthquake interval of approximately 1.0 Ma. The second event occurred between 0.054 and 0.170 Ma, with the mean value of 0.110 Ma. According to both mean ages of these faulting events, recurrence interval between these two events of the minor fault is about 0.900 Ma. This result is also referred to be the recurrence interval of the southeastern segment of the Phrae fault system.

Table 7.1 Slip rate and paleoeartquake magnitude estimation results.

Location	dip angle (degree)	slip length *1 (m)	Age of deposits (million of year)	slip rate *2 (mm/yr)	Maximum displacement, MD (m)	Magnitude*3 (Mw)
CC1	30	3.00	0.054	0.06	1.35	6.8
CC2	35	3.20	0.054	0.06	1.66	6.9
PD2	30	3.10	0.054	0.06	1.39	6.8

*1, slip length = maximum slip length in individual outcrop
*2, slip rate = slip length/age of deposits
*3, magnitude (Mw) = 6.69+0.74*log(MD)

In conclusion, based on this thesis result, recurrence interval of large earthquakes (Mw 6.8-6.9) is 0.900 Ma. In the other word, smaller magnitude earthquakes could be occurred in this area more frequent than the large earthquakes.

Regarding to Fenton et al. (1997), recurrence estimation of the Phrae basin fault (the minor fault in this study) is 12-15 ka, using raw data from the Garbage Landfill outcrop (GL) nearby Ban Pa Deang. This earthquake recurrence result was estimated by dividing slip-per-event by slip rate. The slip-per-event is 1.2-1.5 m and slip rate is 0.1 mm/yr. The slip-per-event was determined from paleoseismic trench excavations and slip rate was calculated from youngest geomorphic feature or stratigraphic unit divided by its relative age. Consequently, uncertainty on slip rate value is at least $\pm$ 50%.

The contrary between this study and Fenton et al. (1997)'s recurrence times is, therefore, emerging from age of faulting events and concept or formula for recurrence calculation. Fenton et al. (1997) calculated recurrence by dividing slip-per-event by slip rate. Slip-per-event is 1.2-1.5 m and slip rate is 0.1 mm/yr. In addition, the age of faulting for calculating slip rate was assumed to be Late Pleistocene (0.01 Ma).

Noteworthy, slip rate and slip-per-event estimation comprise some uncertainties in two folds: (1) field measurement data of the faults and (2) errors in dating offset morphology and stratigraphic units. All of these reasons have also contributed some uncertainties to recurrence estimation (McCalpin, 1996). However, in this thesis, errors in dating are believed to provide more significant for slip rate and recurrence estimations than errors in field data collection.